Broadening, shift and narrowing coefficients in the $2\nu 4$ band of NH3 perturbed by O2, N2 and air

N. Maaroufi, F. Hmida, F. Kwabia Tchana, X. Landsheere, H. Aroui

Broadening, shift and narrowing coefficients in the $2\nu_4$ band of NH_3 perturbed by O_2, N_2 and Air

N. Maaroufi[1, 2*], F. Hmida[1], F. Kwabia Tchana[2], X. Landsheere[2] and H. Aroui[1]

[1]Université de Tunis, Ecole Nationale Supérieure d'Ingénieurs de Tunis, Laboratoire de Spectroscopie et Dynamique Moléculaire, 5 Av Taha Hussein, 1008 Tunis, Tunisia
[2]Laboratoire Interuniversitaire des Systèmes Atmosphériques (LISA), UMR CNRS 7583, Université de Paris, Université Paris-Est Créteil, Institut Pierre-Simon Laplace, 61 avenue du Général de Gaulle, 94010 Créteil Cedex, France

*Corresponding Authors:

Maaroufi Nourhene

Email: nourehenemaaroufi2014@gmail.com

Tel. +216 71496066, Fax. +216 71391166

Keyword: NH_3, $2\nu_4$ band, collisional broadening and shift coefficients, Dicke narrowing parameters, Fourier transform infrared spectroscopy

Abstract

Collisional broadening and shift coefficients as well as Dicke narrowing parameters have been measured at room temperature in the $2\nu_4$ band of NH_3 perturbed by O_2 and N_2 for 310 rovibrational lines with rotational quantum numbers $1 \leq J \leq 11$ and $0 \leq K \leq 11$.

The experiments were performed at room temperature with ammonia mixtures in nitrogen and oxygen at different pressures using a high-resolution Fourier transform spectrometer and a mono-spectrum non-linear least squares fitting of Voigt and soft-collision Galatry profiles. Because of Dicke narrowing effect, departure from the Voigt profile is observed that allowed measurement of narrowing parameters for about 100 transitions of the $2\nu_4$ band. The collisional broadening coefficients obtained with Galatry profile are larger by about 5% than those derived from Voigt profile. Average absolute accuracies of the measurements are estimated to be 5%, 10% and 14% for broadening, shift and narrowing coefficients, respectively.

Air-broadening coefficients were retrieved from the linear combination of O_2- and N_2-broadening coefficients. The results are in good agreement with previous experimental data available in the literature. The whole set of results is given as supplementary material for a possible use in spectroscopic databases.

1. Introduction

Accurate knowledge of ammonia line parameters is necessary for precise interpretation of high-resolution spectra of the Earth's atmosphere and other planetary spaces. Spectroscopic sensors for ammonia are needed for numerous applications including the environment, detection and control of industrial spaces [1], analysis of human breath [2], and recycling of waste-water [3]. Trace detection at ppm levels is often required for these goals [3]. In addition, several laser devices such as rapid-scan absorption [4], wavelength-modulation spectroscopy [5], cavity ring-down [2], and photoacoustic spectroscopy [6] are employed to detect NH_3 traces. Also, NH_3 is an important molecule for astrophysical applications; this interest arises because large quantities of gaseous ammonia have been detected in Jupiter [7] and Saturn [8] conferring to this gas to be a powerful spectroscopic probe of the physico-chemical conditions in the space of these planets. These applications require precise measurements of NH_3 line spectroscopic parameters performed with appropriate experimental setup and the best line models. Furthermore, the NH_3 absorption in Jupiter's atmosphere, especially, has been shown to be highly sensitive to the choice of spectral absorption line shape model [9].

Several experimental and theoretical studies of the line-widths and line shifts in infrared fundamental bands of NH_3 perturbed by several foreign gases were published. However spectroscopy of this molecule is still requested, especially for the overtones and combination bands with the aims to improve spectroscopic databases [10–12] which are largely used for fundamental, planetary, and industrial applications. Among the previous studies, Fabian *et al.* measured O_2, N_2, and Air broadenings for 176 rovibrational lines of NH_3 in the ν_2 band using a high-resolution Fourier Transform Spectrometer (FTS) [13]. The broadenings due to the same perturbers have also been measured and analyzed in the ν_4 band, also, with FTS [14,15]. A prediction of these measurements was achieved with a semi classical model in which the inversion motion of NH_3 is taken into account [16]. Using the same spectrometer, shift coefficients of rovibrational transitions of ammonia perturbed by N_2 and O_2 have been reported in Refs. [17] and [18] respectively.

The temperature dependence of pressure broadening in several branches of the ν_4 and $2\nu_2$ bands of ammonia perturbed by H_2 and N_2 has been measured using a high-resolution FTS [19]. The authors deduced the temperature exponents of the two perturbers. Also, using an FTS, measurements of collision half-widths of NH_3-X (X = H_2, N_2, O_2) systems are reported at three temperatures, lower than 296 K [20]. Air-broadening are deduced at 296 K and the variation of line-widths with rotational quantum numbers J and K was studied. In Ref. [21],

O_2, N_2, Air-broadening and shift parameters of NH_3 in the ν_2 band were measured and analyzed for five lines from spectra recorded with diode-laser spectrometer. Temperature effect of N_2, O_2, CO_2 and H_2O broadening of Q-branch transitions near 10.4 μm were studied in Ref. [22] using two quantum cascade lasers and a multi-line fitting Voigt profile procedure. N_2 and O_2 pressure broadening parameters for some transitions in the $^{R}P(J,0)$ manifold of the $\nu_1+\nu_3$ combination band were measured at room temperature using an external cavity tunable diode laser spectrometer [23].

All previous works neglect the Dicke and speed dependent effects [24–26]; and Voigt line-shapes were used to retrieve the line parameters.

In the 3 μm region, pressure broadening coefficients in the ν_1 and ν_3 bands of NH_3 self-perturbed and perturbed by He, Ar, O_2, N_2, and H_2 were obtained by Markov and Pine [27] using spectra recorded with a difference frequency laser spectrometer. In the low and intermediate pressure range, the authors attributed their fit residual near the line center to the Dicke narrowing.

In Ref. [28] the same authors re-analyze the spectra of Ref. [27] and confront their new results to finer models, which showed clear evidence for Dicke narrowing and speed-dependent effects. A tunable quantum cascade laser was used by Owen *et al*. [29] to measure collisional broadening and Dicke narrowing coefficients of six transitions of NH_3 perturbed by N_2 and O_2 in the spectral region near 1103.46 cm^{-1}. Their analyses were based on Voigt and soft-collision Galatry profiles. In our previous contributions in the $2\nu_4$ band in the 3 μm spectral region [30], we analyzed high-resolution FT spectra with a fitting procedure neglecting Dicke and speed-dependent effects since these effects are greatly masked by the strong long-range interactions of NH_3 with a large dipole moment. These effects, which appear in short range interactions near the line centers, arise mostly at low-pressure domains when collisional and Doppler broadening contributions are comparable.

In the present paper, the broadening and shifting coefficients of the same band perturbed by N_2 and O_2 were measured at room temperature using spectra recorded with a high-resolution FTS. We used a retrieval program based on Voigt and soft-collision Galatry profiles. The pressure broadening and shift coefficients as well as Dicke narrowing coefficients were retrieved. Air-broadening parameters were also determined assuming 79% N_2 and 21% O_2 for the Air composition.

Finally, we compare our results with previous measurements performed in other bands of NH_3 with or without accounting for speed dependence and/or Dicke narrowing [10,13-22,28] for some indications of these effects as well as the vibrational and tunneling dependence of the

broadening parameters. Section 2 briefly describes the spectrometer and the experimental conditions, presents also the fitting procedures and the uncertainty analysis. The measurements of N_2- and O_2-broadening, shift and narrowing coefficients are described in Section 3, which also describes the generation of NH_3-Air broadening coefficients. Comparisons with previous measurements are reported in the same section. Conclusions and remarks are provided in Section 4.

2. Experimental analysis

2.1. Experimental details

Nine spectra of ammonia diluted in oxygen and nitrogen were recorded at a stabilized room temperature of 295 ± 1K in the useful spectral domain from 3100 to 3600 cm^{-1} using the Bruker IFS125HR FTS located at the LISA facility in Créteil (France), the same experimental setup that was used in Ref. [30]. The instrument was equipped with a silicon carbide Globar source, a KBr/Ge beamsplitter, and a liquid nitrogen cooled InSb detector. No optical filter was used. A bandpass of 1900–3800 cm^{-1} is limited by the cut off of the InSb detector (1900 cm^{-1}) and by the electronic filter used (3800 cm^{-1}). The FTS was continuously evacuated below 3×10^{-4} hPa by a turbomolecular pump to minimize absorption by atmospheric gases. The diameter of the entrance aperture of the spectrometer was set to 1.7 mm to maximize the flux of infrared radiation falling onto the InSb detector without saturation or loss of spectral resolution. Interferograms were recorded with a 40 kHz scanner frequency and a maximum optical path difference (MOPD) of 90 cm. According to the Bruker definition (resolution = 0.9/MOPD), this corresponds to a resolution of 0.01 cm^{-1}. Note that the Doppler width is about 0.0096 cm^{-1} at the frequency center of the studied region.

The $^{14}NH_3$, O_2 and N_2 samples were purchased from Sigma Aldrich with stated purities of 99%, 99.99% and 99.98%, respectively. No further sample purification was done. The absorption cell has a base path length of 80 cm and was adjusted for 28 transits in the present experiment, yielding an absorption path length of 2244.9 ± 1.1 cm. The path length includes the distance between the surface of the field mirror and the windows of the cell (2 × 2.45 cm). The sample pressure in the cell was measured using calibrated MKS Baratron capacitance manometers models 628D (2 Torr full scale) and 627D (100 and 1000 Torr full scale), characterized by a stated reading accuracy of 0.12%. Considering the uncertainty arising from small variations of the pressure during the recording of the interferograms (~0.35%), we estimated the measurement uncertainty on the pressure to be equal to 0.5%.

The following procedure was used for the measurements. A background spectrum was first recorded at a resolution of 0.01 cm^{-1} while the cell was being continuously evacuated. The cell was then filled with NH_3 at a given pressure, followed by the perturbing gas (O_2 or N_2) leading to a series of 9 total pressures. One NH_3/O_2 or NH_3/N_2 spectrum was recorded for each NH_3 filling. Transmittance spectra were generated from the ratio of the sample spectra with the background spectrum. The detailed experimental condition is given in Table 1. For the Fourier transform, a Mertz-phase correction with a 1 cm^{-1} phase resolution, a zero-filling factor of 2 and no apodization (boxcar option) were applied to the averaged interferograms, using the procedure included in the Bruker software OPUS package [31,32]. The peak-to-peak signal-to-noise ratio (S/N) in the ratioed spectra is around 800. The spectra were calibrated by matching the measured positions of 37 lines of residual H_2O in the FTS observed therein to reference wavenumbers available in HITRAN [10] with an RMS deviation of 0.00018 cm^{-1}. The calibration factor was determined with the H_2O positions measured in the NH_3 spectrum at lower pressure and then applied to all other spectra.

Table 1: Experimental conditions and pressures used to record the $2\nu_4$ band of NH_3 perturbed by O_2 and N_2.

Experimental conditions					
Resolution (cm^{-1})			0.01		
Maximum optical path difference (cm)			90		
Diaphragm diameter (mm)			1.7		
Focal distance (mm)			418		
Optical cell length (cm)			2244.9		
Useful spectral domain (cm^{-1})			3100 - 3600		
Spectrum number and pressures					
#	NH_3 pressure (Torr)	N_2 pressure (Torr)	#	NH_3 pressure (Torr)	O_2 pressure (Torr)
S1	0.0809(4)	19.94(10)	S1	0.0803(4)	20.46(10)
S2	0.1624(8)	40.02(20)	S2	0.1604(8)	39.94(20)
S3	0.2420(12)	59.97(30)	S3	0.2431(12)	60.52(30)
S4	0.3243(16)	80.00(40)	S4	0.3216(16)	80.01(40)
S5	0.4005(20)	100.0(5)	S5	0.3975(20)	99.70(50)
S6	0.4802(24)	119.9(6)	S6	0.4828(24)	121.1(6)
S7	0.7990(40)	160.0(8)	S7	0.8003(40)	160.3(8)
S8	1.1981(60)	239.8(12)	S8	1.1969(60)	240.1(12)
S9	1.5032(75)	300.0(15)	S9	1.4950(75)	299.9(15)

2.2. Data analysis and fitting procedure

Generally, to measure the self-broadening for molecules with large dipole moment, the Dicke and speed-dependent effects can be neglected since they are masked by the strong long-range interactions between molecules. Here, since the ammonia perturbed by oxygen and nitrogen, are rather short range collisions, these effects should be taken into account since at low pressure range, the mean-free path of molecules decreases as the pressure increases to become

smaller than the light wavelength, implying a reduction of the Doppler width [24] and narrower profile (Dicke effect). Therefore, we used the following soft-collision Galatry profile [26] which is based on diffusion model.

$$G(\sigma-\sigma_0)=\frac{A}{\sqrt{\pi}}\mathrm{Re}\left[\frac{1}{(1/2z)+y-ix}\times M\left(1;1+\frac{1}{2z^2}+\frac{y-ix}{z};\frac{1}{2z^2}\right)\right] \quad (1)$$

$M(\ldots;\ \ldots;\ \ldots)$ is the hypergeometric function; x and y are the Doppler normalized shift and pressure broadening given by:

$$A=\frac{S\sqrt{Ln2}}{\gamma_D\sqrt{\pi}}\quad,\quad x=\sqrt{Ln2}\frac{\sigma-\sigma_0}{\gamma_D}\quad,\quad y=\sqrt{Ln2}\frac{\gamma}{\gamma_D} \quad (2)$$

In these equations, S is the line intensity in cm^{-2}, σ_0 its wavenumber in cm^{-1} including the collisional shift, γ and γ_D in cm^{-1} are the collisional and Doppler line half-widths respectively. The normalized parameter z is related to the collisional narrowing β in cm^{-1} (also called the dynamical friction parameter) by:

$$z=\sqrt{\ln 2}\frac{\beta}{\gamma_D} \quad (3)$$

Note that when $z = 0$, the Galatry profile is reduced to the Voigt profile.

The recorded nine spectra were simulated by Voigt and soft-collision Galatry profiles using a mono-spectrum fitting procedure which allows to retrieve line parameters of $2\nu_4$ band of NH_3. This procedure uses the WSpectra code [33] based on a non-linear least-square method in which line position, intensity, width, background, and the narrowing parameter were determined by adjusting a synthetic transmittance to minimize the residual between the observed and simulated profiles. Only the three first parameters are derived from the fit with Voigt profile. Note that in the two fitting procedures, the Doppler width was fixed to its calculated value.

Figure 1 illustrates an example of the measured line shape of the ${}^{Q}{}_{s}R(6,3)$, ${}^{Q}{}_{a}R(7,5)$ and ${}^{Q}{}_{a}R(5,3)$ transitions and the calculated profiles described either by the basic Voigt profile or by the Galatry model. The two profiles are quite similar and thus difficult to distinguish on the same plot. The residuals given at the bottom, resulting from the difference between the measured and the calculated profiles show an evident improvement in the fitting obtained

when the Dicke narrowing is taken into account through the Galatry profile. When the Voigt profile is used, one can observe a W-shape residuum characteristic of line narrowing. Examination of differences between the observed and calculated spectra shows that these residuals are generally less than 1%.

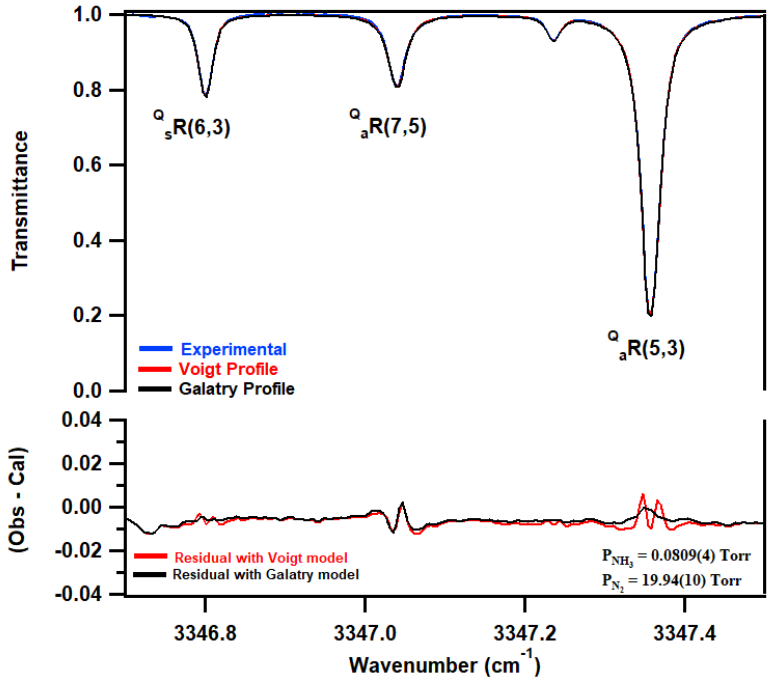

Figure 1: Experimental line shape of the $^{Q}_{s}R(6,3)$, $^{Q}_{a}R(7,5)$ and $^{Q}_{a}R(5,3)$ transitions in the $2\nu_4$ band of NH_3 perturbed by N_2 recorded at P_{NH3}= 0.0809 and P_{N2}=19.94 Torr, fitted with Galatry and Voigt profiles; (Obs-cal) shows the residuals using either Voigt or Galatry models.

2.3. Uncertainty analysis

In the following, the measured values of line broadening and shift coefficient as well as narrowing coefficients are presented with their absolute accuracies estimated from uncertainties on all physical parameters, standard deviation of the fit and contributions from possible systematic errors. Assuming these parameters are uncorrelated quantities, the estimation of each transition accuracy can be calculated as [34]:

$$\varepsilon = \sqrt{\varepsilon_{si}^{\,2} + \varepsilon_{t}^{\,2} + \varepsilon_{p}^{\,2} + \varepsilon_{fit}^{\,2} + \varepsilon_{sys}^{\,2}} \qquad (4)$$

In this equation ε_{si} =1%, ε_t = 0.34% and ε_p= 0.5% are the uncertainties associated with the sample purity, the temperature, and the pressure, respectively. ε_{fit} and ε_{sys} are the uncertainties of the standard deviation of the fit and the systematic errors. The dominant contributions to

systematic errors arise from the location of the full-scale photometric level, channeling, as well as electronic and detector nonlinearities [34,35]. A realistic assessment of systematic errors is not an easy task and probably strongly depends on the setup used. Our present estimate is based upon the arguments developed in Ref. [34] using instruments comparable to ours. We retained 4% as the contribution of systematic errors on retrieved parameters. It is an arbitrary, but conservative value. These various uncertainties evaluated for the broadening coefficients are given in Figure 2 for 5 selected lines, representative of the 310 measured lines, i.e. $^{P}_{a}P(3,3)$, $^{P}_{a}P(4,3)$, $^{P}_{a}P(5,3)$, $^{P}_{a}P(6,3)$ and $^{P}_{a}P(7,3)$. We can observe that the systematic errors and the standard deviation from the linear fit are the main sources of errors. Considering these various sources of errors, we estimate that, on average, accuracies of the measurements are 5% for broadening coefficients, 10% for shift coefficients and 14% for narrowing coefficients.

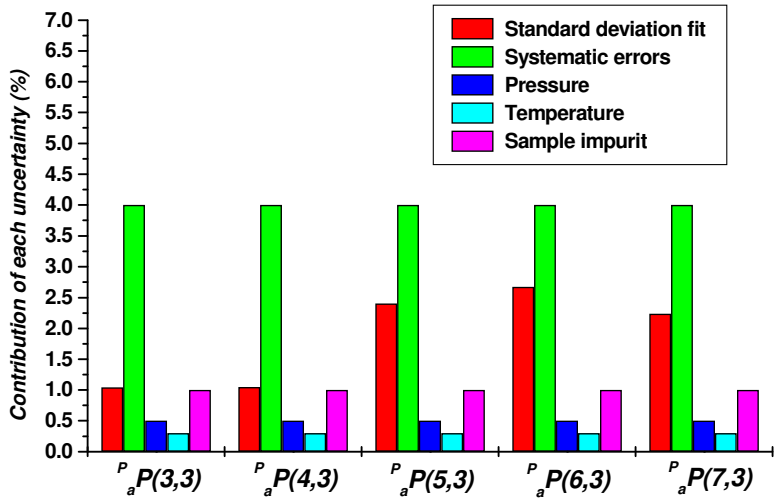

Figure 2: Comparison between various sources of relative uncertainty on the measured O_2 -broadening coefficients for 5 selected lines: $^{P}_{a}P(3,3)$, $^{P}_{a}P(4,3)$, $^{P}_{a}P(5,3)$, $^{P}_{a}P(6,3)$ and $^{P}_{a}P(7,3)$.

3. Results and discussion

3.1. Broadening coefficients

In collisions between ammonia and the homopolar molecules, nitrogen and oxygen, dipole–quadrupole interaction becomes somewhat dominant, but significantly smaller than the strong long-range interactions of NH_3 self-collision. Then the self-broadening must be considered while determining the foreign-gas-broadened line-widths.

Although the spectra of the NH_3-O_2 and NH_3-N_2 mixtures were recorded with at most 0.5% of NH_3, we subtracted the self-broadening contributions to deduce, at the best, the N_2- and O_2-coefficients, according to the equation:

$$\gamma = \gamma_{0O_2/N_2} P_{O_2/N_2} = \gamma_{total} - \gamma_{0Self} P_{NH_3} \quad (5)$$

where γ is the N_2- or O_2-collisional half-width in cm^{-1}, γ_{total} is the total collisional half-width in cm^{-1}, and P_{NH_3} and P_{O_2/N_2} are the NH_3 and O_2 or N_2 partial pressures in atm respectively. γ_{0O_2/N_2} is the N_2- or O_2-broadening coefficients and γ_{0Self} is the self-broadening coefficient taken from Ref. [30]. The evolution with the O_2 pressure of γ measured for the $^{Q}_{a}R(3,1)$ line obtained from the Voigt and Galatry fits is shown in Figure 3.

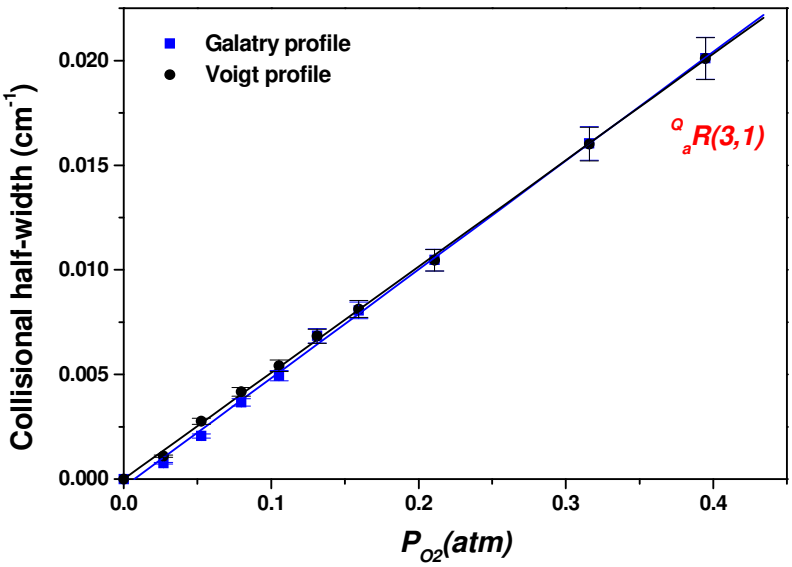

Figure 3: Collisional half-widths of the $^{Q}_{a}R(3,1)$ transition versus the O_2 pressure. Data are derived from Voigt (black circle symbols) and Galatry (blue square symbols) profiles. The linear fits are used to retrieve the O_2-broadening coefficient in units of $cm^{-1}.atm^{-1}$.

This figure shows the linear dependence of the collisional half-widths with pressure for the two models. The O_2-broadening coefficients (in $cm^{-1}.atm^{-1}$) were derived from the slopes of these lines. The results of line broadening and shift coefficients as well as narrowing coefficients, all in the unit of $cm^{-1}.atm^{-1}$, along with their absolute uncertainties are given in the supplementary material listing 310 lines of the $2\nu_4$ band. Table 2 illustrates a sample of these results for $^{P}_{s}P(5,K)$ manifold. Three remarks can be addressed about the trends of broadening coefficients:

- they indicate no systematic inversion symmetry dependence;

- they increase with *K* for a given *J* and decrease with *J* for a fixed *K*;

- in most cases, values retrieved from Galatry profile are relatively higher than the ones derived from Voigt profile by about 5%.

The first two remarks are the same as those observed for self-broadening in Ref. [16,19,20,30].

The measured values range from 0.0458 to 0.1812 $cm^{-1}.atm^{-1}$ for N_2 perturber and from 0.0318 to 0.0753 $cm^{-1}.atm^{-1}$ for O_2 perturber.

Table 2: Measured N_2-, O_2- and Air-broadening, narrowing and shift coefficients in $cm^{-1}.atm^{-1}$ at 295 K for five transitions of the $^{P}_{s}P(5,K)$ manifold retrieved with Voigt profile (VP) and Galatry profile (GP). All the uncertainties are calculated using Eq. (4).

Transition	Position[(a)]	Profile	γ_0 ($cm^{-1}.atm^{-1}$)		$\gamma_{0\,Air}$ ($cm^{-1}.atm^{-1}$)	β_0 ($cm^{-1}.atm^{-1}$) [(b)]		δ_0 ($cm^{-1}.atm^{-1}$) [(c)]	
			NH_3-O_2	NH_3-N_2	NH_3-Air	NH_3-O_2	NH_3-N_2	NH_3-O_2	NH_3-N_2
$^{P}_{s}P(5,1)$	3154.334810	VP	0.0491 ± 0.0032	0.0799 ± 0.0036	0.0815 ± 0.0043	0.0196 ± 0.0047	0.0641 ± 0.0166	-0.0046 ± 0.0004	-0.0081 ± 0.0008
		GP	0.0525 ± 0.0024	0.0892 ± 0.0048					
$^{P}_{s}P(5,2)$	3166.726590	VP	0.0511 ± 0.0039	0.0863 ± 0.0038	0.0927 ± 0.0041	0.0109 ± 0.0018	0.0324 ± 0.0044	-0.0052 ± 0.0004	-0.0051 ± 0.0006
		GP	0.0519 ± 0.0024	0.1035 ± 0.0045					
$^{P}_{s}P(5,3)$	3177.714610	VP	0.0537 ± 0.0032	0.0914 ± 0.0039	0.0878 ± 0.0038	0.0147 ± 0.0017	0.0351 ± 0.0022	-0.0044 ± 0.0004	
		GP	0.0541 ± 0.0029	0.0967 ± 0.0040					
$^{P}_{s}P(5,4)$	3188.554070	VP	0.0551 ± 0.0030	0.0954 ± 0.0041	0.0941 ± 0.0042	0.0132 ± 0.0012	0.0342 ± 0.0049	-0.0050 ± 0.0003	-0.0058 ± 0.0005
		GP	0.0558 ± 0.0026	0.1043 ± 0.0046					
$^{P}_{s}P(5,5)$	3195.033800	VP	0.0543 ± 0.0029	0.0912 ± 0.0039	0.0938 ± 0.0043	0.0110 ± 0.0022	0.0236 ± 0.0024	-0.0058 ± 0.0005	-0.0043 ± 0.0003
		GP	0.0552 ± 0.0027	0.1040 ± 0.0047					

(a) Line positions are from HITRAN.[10]
(b) O_2 - and N_2 -narrowing coefficients obtained with Galatry model.
(c) O_2 - and N_2 -shift coefficients obtained with Galatry model.

The rotational trends of the broadening coefficients of the two foreign gases are illustrated in Figure 4 for the ^{P}P sub-branch. The variation of these coefficients with *J* for each *K* is shown in Figures 4a and 4c, whereas, we show the variation with *K* for each *J* in Figures 4b and 4d. The plots for N_2-broadening (Figures 4a, 4b) and Air-broadening (not shown here) appear to be convex, while they are roughly concave for O_2-broadening (Figures 4c, 4d).

Since this work reports the data of N_2- and O_2-broadening coefficients in the $2\nu_4$ band for the first time, comparison of values listed in Table 2 and supplementary material will be done with those performed in other bands in Refs. [14,15,20-22,28].

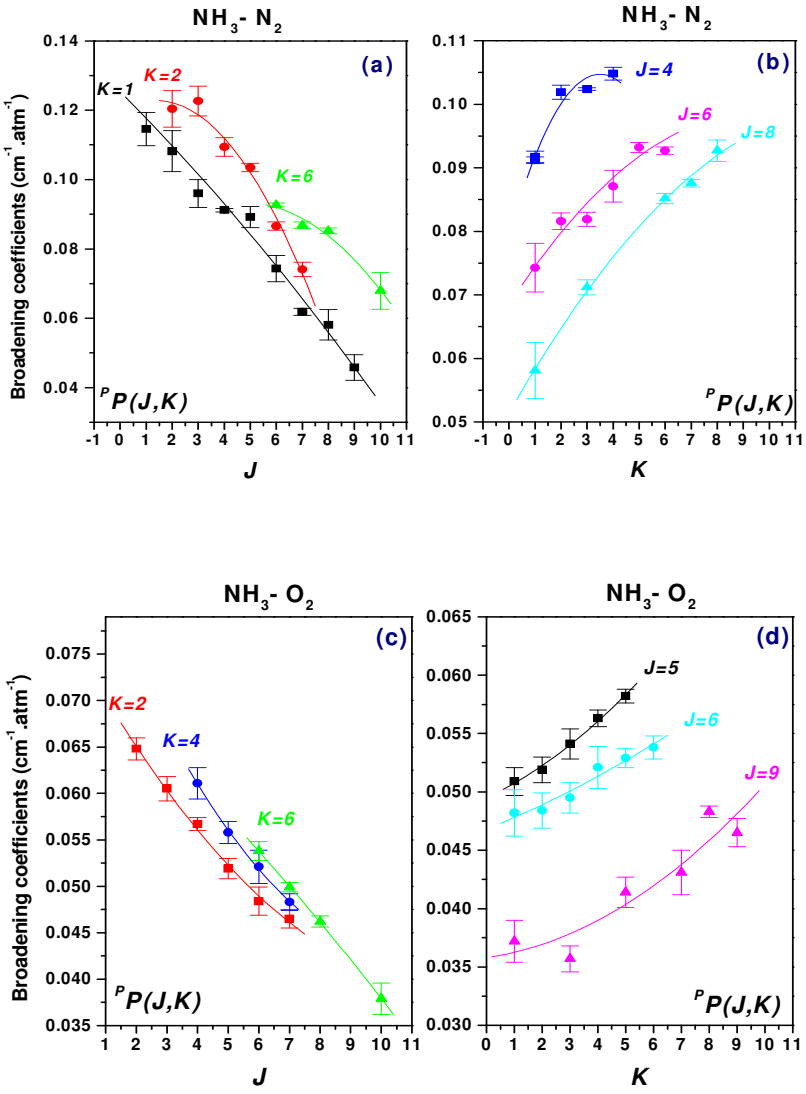

Figure 4: Variation of N_2- and O_2 -broadening coefficients ($cm^{-1}.atm^{-1}$) in $2\nu_4$ band of NH_3 with J and K in the ^{P}P sub-branch at 295 K.

For broadening coefficients, the values retrieved from the Galatry profile, differ by about 2% and 4% for O_2 and N_2 perturbers respectively from the values taken from Pine et *al.* [28] for 63 lines studied in common. These data were obtained mostly in the Q- and R-branch of the ν_1 band. Also, we compared our data with those in the ν_2 band reported in Ref. [20] also obtained with a FTS using the same spectral resolution of 0.01 cm^{-1} as the present experiment. Our data agreed within 5% for most of the lines reported in this reference. In the same band, O_2- and N_2-broadening coefficients in Ref. [21] agree with our data within 2% and 5% for O_2 and N_2 perturbers respectively. When the present values were compared with those reported in Ref. [22] for N_2-broadening in the Q-branch of the ν_2 band, the agreement is less satisfactory with a difference of about 10%. This difference is reduced to 4% if we compare

our O_2-broadening data with those reported in the same reference. Moreover, our results are in excellent agreement with the values obtained in Refs. [14,15]; the average difference is about 2% for O_2 and N_2 perturbers.

3.2. Collisional narrowing parameters

The Dicke parameters, β, are measured within the spectra adjusted by the Galatry profile that includes the narrowing confinement parameter arising from velocity changing collisions. In our fitting procedure, these effects occur at low pressure and we observed a convergence of the Galatry fit with positive values of this parameter for all transitions for which this narrowing is observed. Note that in the observed line profiles these effects can occur themselves as a shift of amplitude transmittance at the line center when a Voigt profile is used.

Collisional narrowing coefficients β_0 for NH_3 perturbed by O_2 and N_2 were derived from the plots of the parameter β as a function of the gas pressure. The slope of the straight-line gives the coefficient β_0. A typical plots of β versus P are presented in Figure 5 for the ${}^{Q}{}_{a}R(5,3)$ and ${}^{P}{}_{s}P(5,3)$ transitions which show a good linearity of β with the pressure.

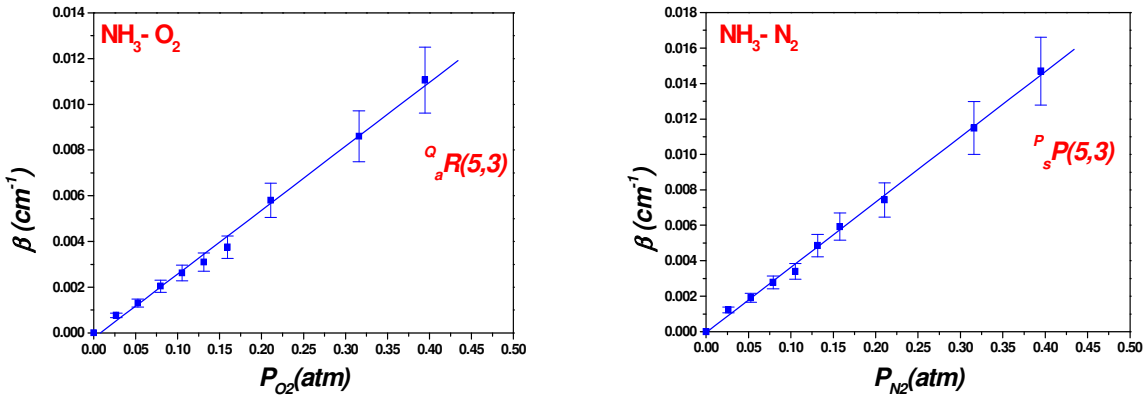

Figure 5: Narrowing parameter β of the ${}^{Q}{}_{s}R(5,3)$ and ${}^{P}{}_{a}P(5,3)$ transitions in the $2\nu_4$ band of NH_3 versus the pressure retrieved with the Galatry profile. The corresponding β_0 coefficient is deduced from the slope of the linear fit.

Numerous weak and/or blended lines illustrate significant dispersion of points in the graph of β versus the pressure, so it does not allow to determine any slope. Consequently, the measurement of the narrowing coefficients β_0 was only possible for 120 transitions for O_2 perturber and 100 transitions for N_2 one. The values of these coefficients with their uncertainties determined by Eq. (4) are listed in Table 2 and in the supplementary material,

and are shown in Figure 6 versus *K* for all values of *J*, illustrating an agreement with Refs. [28] and [29], which report data for the ν_1 and ν_2 bands respectively. The average values are 0.0226 and 0.0357 $cm^{-1}.atm^{-1}$ for O_2 and N_2 respectively. The corresponding accuracies are about 14% for the two perturbers.

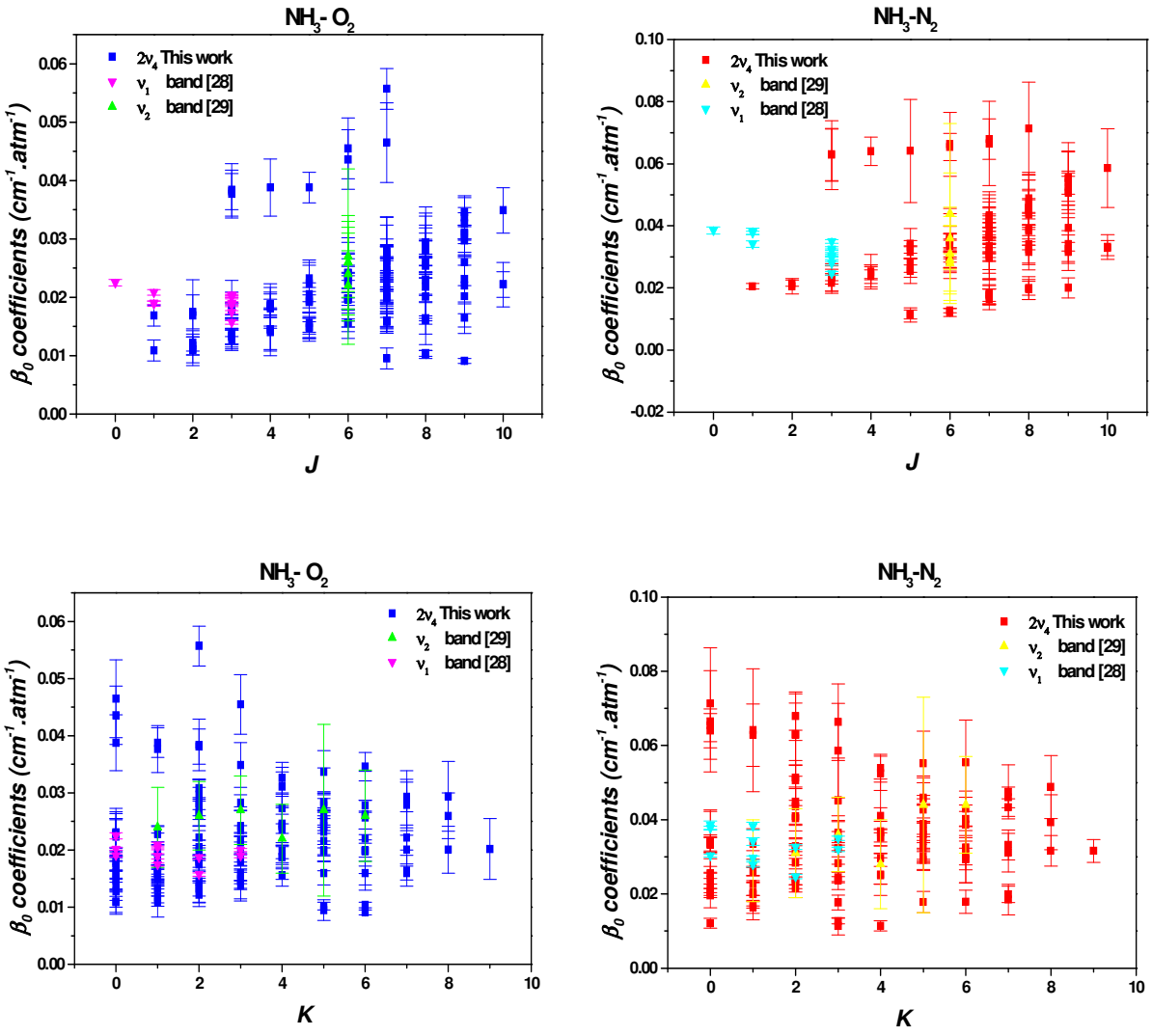

Figure 6: Narrowing coefficients β_0 in $cm^{-1}.atm^{-1}$ in the $2\nu_4$ band of NH_3 at 295 K obtained with Galatry model as function of quantum numbers J and K. Measured values of Pine et al. [28] and Owen et al. [29] are also plotted for comparison.

It is difficult to measure the narrowing parameters with high precision since they are generally small. Two reasons can be addressed; firstly, it may be related to the strong correlation between the broadening and narrowing parameters [36]; secondly, it concerns the difficulty of observing fine effects such as Dicke collisional narrowing and speed-dependent using Fourier transform spectroscopy.

The measured collisional narrowing coefficients can be compared to those measured in the ν_1 band in Ref. [28] using the Galatry model. This reference reported an average values of 0.0226 ± 0.0029 $cm^{-1}.atm^{-1}$ for NH_3-O_2 mixture and 0.0357 ± 0.0051 $cm^{-1}.atm^{-1}$ for NH_3-N_2 one. Owen *et al.* [29] measured line narrowing coefficients β_0 when fitting ro-vibrational lines of the ${}_sR(6,K)$ manifold in the ν_2 band of NH_3 mixed with O_2 and N_2. The average values on studied transitions are listed in Table 3 which illustrates a reasonable agreement between narrowing parameters measured in different wavenumber regions in the ν_1 [28], ν_2 [29] and $2\nu_4$ bands. The largest difference is observed for N_2 with a value of 12% between the present work and Ref. [28] for O_2 the agreement is better with a difference of about 7%. When we compare with those of the ν_2 band [29], our value for N_2 is in perfect agreement, but we found a difference of about 11% for O_2. These differences appear to be large but are in the margin of errors of Ref. [29], which are about 41% and 32% for N_2 and O_2 respectively; those of the present work are 14% and 13% for N_2 and O_2 respectively. The two last uncertainties account for all sources of errors, while that of Ref. [28], 1% for the two perturbers, is equal to the standard deviation. Considering these uncertainties, we can state a reasonable agreement between these works.

Table 3: Average narrowing coefficients β_0 in $cm^{-1}.atm^{-1}$ measured for NH_3 perturbed by N_2 and O_2 with the Galatry model. Data are compared with measurements of Refs. [28,29].

	$\beta_{0\ NH3\text{-}N2}$	$\beta_{0\ NH3\text{-}O2}$
This work	0.0357 ± 0.0051	0.0226 ± 0.0029
Pine *et al.*[28]	0.0412 ± 0.0003	0.0243 ± 0.0002
Owen *et al.* [29]	0.0353 ± 0.0145	0.0253 ± 0.0080

Our values of β_0 allow to calculate the optical diffusion constants D_{diff} of the NH_3-O_2 and NH_3-N_2 mixtures using the formula:

$$D_{diff} = \frac{kT}{2\pi cM\,\beta_0} \tag{6}$$

where $k = 1.38064852\times10^{-23}\ J.K^{-1}$ is the Boltzmann constant, T is the temperature of the mixture, c is the speed of light and M is the mass of the absorbing molecule. We found 0.218 $cm^2.s^{-1}$ and 0.347 $cm^2.s^{-1}$ for NH_3-O_2 and NH_3-N_2 binary mixture, respectively. When comparing these values with Ref. [37], we found an excellent agreement for N_2 with a difference of 1%, but a large discrepancy (≈ 34%) is observed for O_2. This reference reported

the values 0.220 ± 0.005 $cm^2.s^{-1}$ and 0.227 ± 0.004 $cm^2.s^{-1}$ for NH_3-O_2 and NH_3-N_2 binary mixture, respectively.

3.3. O_2 and N_2 pressure-induced shift coefficients

The pressure shifts are generally much smaller than the widths and are difficult to measure with high accuracy. The pressure-induced shift coefficients δ_0 in $cm^{-1}.atm^{-1}$ of O_2- and N_2-perturber were determined using the following expression:

$$\sigma_0 = \sigma_{00} + \delta_0 P_{N_2/O_2} \quad (7)$$

where σ_{00}, in cm^{-1}, is the unperturbed wavenumber and σ_0 (cm^{-1}) the line position corresponding to a given total pressure. A typical plot of the collisional wavenumber σ_0 as a function of the pressure $P_{N2/O2}$ is shown in Figure 7.

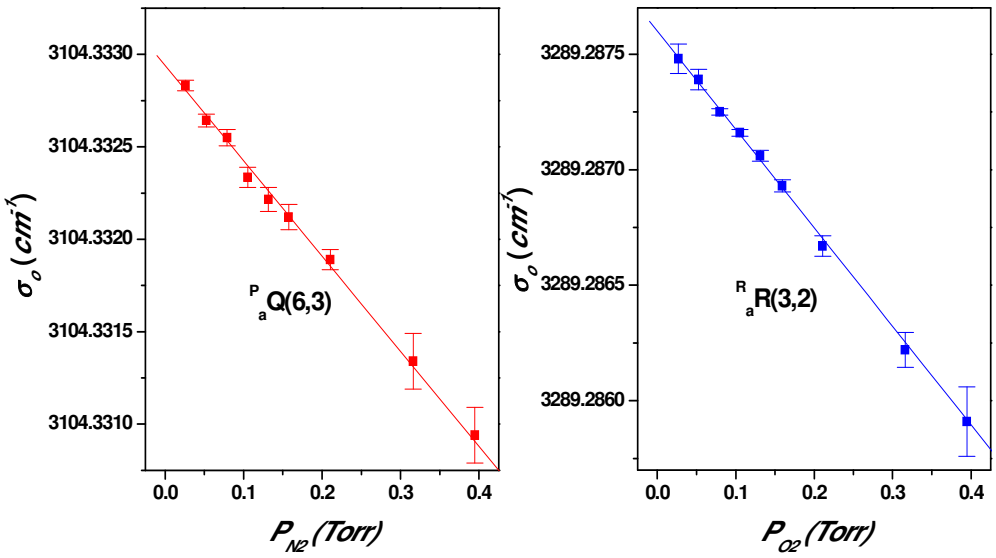

Figure 7: Dependence of measured wavenumber σ_0 with the N_2 and O_2 partial pressures P_{N2} and P_{O2} for the $^{P}_{a}Q(6,3)$ and $^{R}_{a}R(3,2)$ lines. The collisional line shift coefficient δ_0 is derived from the slope of the best fit line. (■) correspond to experimental data and solid line to the linear regression.

The straight line obtained from the fitting illustrates the linearity of the measured wavenumber against pressure for the $^{P}_{a}Q(6,3)$ and $^{R}_{a}R(3,2)$ lines in the $2\nu_4$ band of NH_3. Note that due to the low pressure values of NH_3 ($\leq 0.5\%$ of the total pressure), the self-shifts were neglected.

The N_2- and O_2-shift coefficients δ_0, in $cm^{-1}.atm^{-1}$, are derived from the slope of these straight lines. The whole set of the data shift for the two buffer gases are listed in the supplementary material, and few transitions are collected in Table 2, together with their absolute uncertainty estimated using Eq. (4).

Figure 8 shows a comparison of our experimental shift coefficients δ_0 for the $2\nu_4$ band perturbed by O_2 with the values obtained for the ν_1 band of NH_3 in Ref. [27] and those of the ν_4 band in Ref. [18]. This figure and supplementary material illustrate an excellent agreement, with an average difference of about 3% with Ref. [27] and about 2% with Ref. [18]. For the NH_3-N_2 system, we obtain an average difference of 6% with Ref. [27], and 8% with Ref. [17]. All the O_2 shift coefficients are negative illustrating a decrease of line position with pressure. They vary between -0.0020 and -0.0267 $cm^{-1}.atm^{-1}$ with an average value of -0.0061 $cm^{-1}.atm^{-1}$. For N_2, 12 transitions out of 155 lines have positive shifts; they range from -0.0551 and 0.0303 $cm^{-1}.atm^{-1}$ with a mean value of -0.0059 $cm^{-1}.atm^{-1}$. The same trend of signs is observed by Pine *et al.* in Ref. [27] and Dhib *et al.* in Ref. [17]. These shifts do not exhibit any distinguishable J and K dependences. On the other hand, we can also observe a satisfactory agreement between our values and those of Refs. [27] and [17,18] for the ν_1 and ν_4 band respectively, indicating that they are insensitive to vibrational excitation.

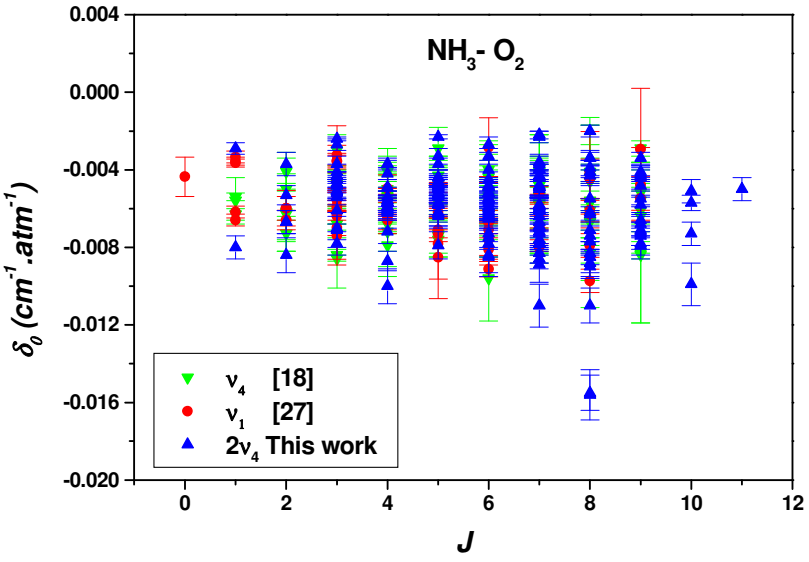

Figure 8: Comparison of our values of O_2 -shift coefficients δ_0 obtained in the $2\nu_4$ band of NH_3 with results obtained by Pine et al. in the ν_1 band [27] and Aroui et al. in the ν_4 band [18].

3.4. Air-broadening coefficients

Since N_2 and O_2 are the major constituents of the Earth's atmosphere, it is possible to determine Air-broadening coefficients from the values for nitrogen- and oxygen-broadening given in the supplementary material using the following equation:

$$\gamma_{0Air} = 0.79\times\gamma_{0N2} + 0.21\times\gamma_{0O2} \quad (8)$$

The derived values of the Air-broadening coefficients range from 0.0434 to 0.1544 $cm^{-1}.atm^{-1}$. These coefficients are listed for a few transitions in Table 2. The whole set of these coefficients is presented in the supplementary material.

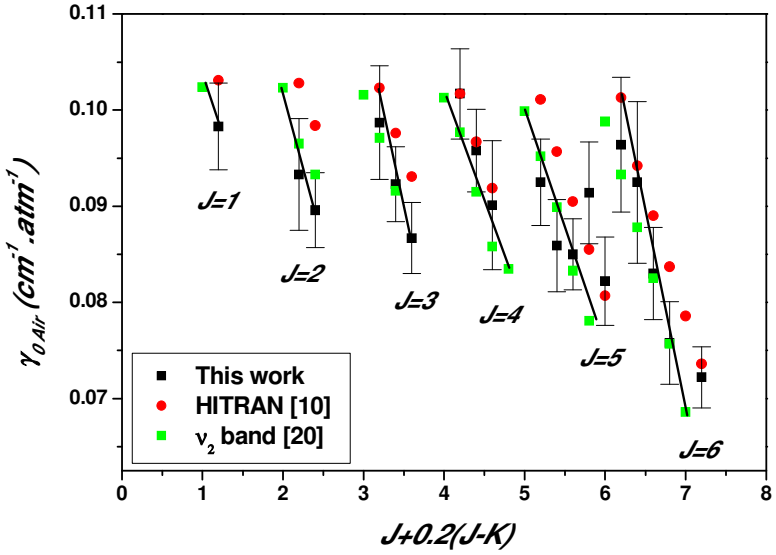

Figure 9: Air-broadening coefficients in the $2\nu_4$ band of NH_3 at 295 K as function of J+0.2(J-K) for the manifolds J=1→ 6. Values from Refs. [10,20] are also plotted.

The present results of Air-broadening coefficients reproduce the systematic *J* and *K* quantum numbers dependencies of Refs. [10,13,20] namely a decrease as a function of *J* for a fixed *K* and an increase versus *K* for a given *J*. It is illustrated in Figure 9 for the ${}^{Q}P$ and ${}^{R}R$ sub-branches of the $2\nu_4$ and ν_2 bands, respectively. The Air-broadening coefficients of HITRAN [10] derived from the polynomial model of ν_2 band measurements of Nemtchinov *et al.* [20], the difference with previous works are about 6% when the present data are compared to those of the ν_2 band of Ref. [20].

4. Conclusions

This work presents the first measurements of pressure broadening and shift coefficients as well as narrowing coefficients for 310 transitions in the $2\nu_4$ band of NH_3 perturbed by N_2 and O_2 at 295 K in the 3100 - 3600 cm^{-1} spectral region. Voigt and soft-collision Galatry profiles were used to fit the measured line shape of each individual transition at various pressures. For a significant number of transitions, deviations from the Voigt profile were observed, highlighting the Dicke narrowing effect. We have quantified this effect for more than 100 lines, thanks to the high signal-to-noise ratio obtained in our Fourier Transform spectra. In all cases, Galatry model gives slightly higher values compared to Voigt one. Our data are compared with previous work when it's possible.

Using the measured broadening coefficients of the NH_3-O_2 and NH_3-N_2 systems, we have produced the NH_3 Air-broadening coefficients that were also compared with data in the literature. The measured narrowing and shift coefficients are consistent with the rare previous works in the literature for other bands. The data obtained in this work are available for use in the HITRAN and GEISA databases.

Acknowledgment: The authors are grateful to Dr. J. Vander Auwera from the Université Libre de Bruxelles for making available his fitting program.

References

[1] Schilt S, Thévenaz L, Niklès M, Emmenegger L, Hüglin C. Ammonia monitoring at trace level using photoacoustic spectroscopy in industrial and environmental applications. Spectrochim Acta Part A Mol Biomol Spectrosc 2004;**60**:3259–68.

[2] Manne J, Sukhorukov O, Jäger W, Tulip J. Pulsed quantum cascade laser-based cavity ring-down spectroscopy for ammonia detection in breath. Appl Opt 2006;**45:**9230.

[3] Webber ME, Claps R, Englich FV, Tittel FK, Jeffries JB, Hanson RK. Measurements of NH_3 and CO_2 with distributed-feedback diode lasers near 2.0 μm in bioreactor vent gases. Appl Opt 2001;**40**:4395.

[4] Claps R, Englich FV, Leleux DP, Richter D, Tittel FK, Curl RF. Ammonia detection by use of near-infrared diode-laser-based overtone spectroscopy. Appl Opt 2001;**40**: 4387–94.

[5] Owen K, Farooq A. A calibration-free ammonia breath sensor using a quantum cascade laser with WMS 2f/1f. Appl Phys B 2013;**116**:371–83.

[6] Filho MB, da Silva MG, Sthel MS, Schramm DU, Vargas H, Miklós A and *al.* Ammonia detection by using quantum-cascade laser photoacoustic spectroscopy. Appl Opt 2006;**45**:4966–71.

[7] Kunde V, Hanel R, Maguire W, Gautier D, Baluteau JP, Marten A, Chedin A, Husson H, and Scott NS, J Astrophys 1982;**263**:443–67.

[8] Ho PTP and Townes CH, Ann Rev Astron Astrophys 1983;**21**:239–70.

[9] Encrenaz T and Moreno R. The microwave spectra of planets, in: AIP Conference Proceedings – Experimental cosmology at millimetre wavelengths: 2K1BC Workshop. 2002;**616**:330–37.

[10] Gordon IE, Rothman LS, Hill C, Kochanov RV, Tan Y, Bernath PF and *al.* The HITRAN 2016 molecular spectroscopic database. JQSRT 2017;**203**:3-69.

[11] Jacquinet-Husson N, Scott NA, Chedin A, Crepeau L, Armante R, Capelle V *et al.* The 2009 edition of the GEISA spectroscopic database. JQSRT 2011;**112**:2395-445.

[12] Pickett HM, Poynter RL, Cohen EA, Delitsky ML, Pearson JC, Muller HSP. Submillimeter, millimeter, and microwave spectral line catalog. JQSRT 1998;**60**: 883-90.

[13] Fabian M. Ito F and Yamada KMT. N_2, O_2, and Air broadening of NH_3 in ν_2 band measured by FTIR Spectroscopy. J Mol Spectrosc 1995;**173**:591–602, corrected later in 2006 in J of Mol Spectros 2006;**236**:150.

[14] Aroui H, Chevalier M, Broquier M, Picard-Bersellini A, Gherissi S, Legay Sommaire N. Line mixing parameters in the ν_4 rovibrational band of NH_3 perturbed by N_2. J Mol Spectrosc 1995;**169**:502–10.

[15] Aroui H, Broquier M, Picard-Bersellini A, Bouanich JP, Chevalier M, Guerissi S. Absorption intensities, pressure-broadening and line mixing parameters of some lines of NH_3 in the ν_4 band. JQSRT 1998;**60**:1011–23.

[16] Dhib M, Bouanich JP, Aroui H, Picard-Bersellini A. Analysis of N_2, O_2, CO_2, and Air broadening of infrared spectral lines in the ν_4 band of NH_3. JQSRT 2001;**68**:163–78.

[17] Dhib M, Aroui H, Orphal J. Experimental and theoretical study of line shift and mixing in the ν_4 band of NH_3 perturbed by N_2. JQSRT 2007;**107**:372-84.

[18] Aroui H, Chelin P, Echargui MA, Fellows CE, Orphal J. Line shifts in the ν_2, $2\nu_2$ and ν_4 bands of NH_3 perturbed by O_2. J Mol Spectrosc 2008;**252**:129-35.

[19] Nouri S, Orphal O, Aroui H and Harmann JM. Temperature dependence of pressure broadening of NH_3 perturbed by H_2 and N_2 .J Mol Spectrosc 2004;**227**:60-66.

[20] Nemtchinov V, Sung K,Varanasi P. Measurements of line intensities and half-widths in the10-μm bands of $^{14}NH_3$. JQRST 2004;**83**:243–65.

[21] Dhib M, Ibrahim N, Chelin P, Echargui M.A, Aroui H, Orphal J. Diode-laser measurements of O_2, N_2 and Air-pressure broadening and shifting of NH_3 in the 10 µm spectral region. J Mol Spectrosc 2007;**242**:83–89.
[22] Sur R, Spearrin RM, Peng WY, Strand CL, Jeffries JB, Enns GM, Hanson RK. Line intensities and temperature-dependent line broadening coefficients of Q-branch transitions in the ν_2 band of ammonia near 10.4 µm. JQSRT 2016;**175**:90-99.
[23] Koshelev MA, Tretyakov MY, Lees RN, Xu LH. ECTDL study of N_2- and O_2-pressure broadening of a series of ammonia lines in the 1.5 µm (ν_1+ν_3) combination band. Appl Phys B 2006;**85**:273-77.
[24] Dicke RH. The effect of collisions upon the Doppler width of spectral Lines. Phys Rev 1953;**89**:472–3.
[25] Rautian SG, Sobelman II. The effect of collisions on the Doppler broadening of spectral lines. Sov phys Uspheki 1967;**9**:701–16.
[26] Galatry L. Simultaneous effect of Doppler and foreign gas broadening on spectral lines. Phys Rev 1961;**122**:1218–23.
[27] Pine AS, Markov VN, Buffa G, Tarrini O. N_2, O_2, H_2, Ar and He broadening in the ν_1 band of NH_3. JQSRT 1993;**50**:337–48.
[28] Pine AS, Markov VN. Self and foreign-gas-broadened line shapes in the ν_1 band of NH_3. J Mol Spectrosc 2004;**228**:121-42.
[29] Owen K, Es-sebbar E-t, Farooq A. Measurements of NH_3 line strengths and collisional broadening coefficients in N_2, O_2, CO_2, and H_2O near 1103.46cm^{-1}. JQSRT 2013;**121**:56–68.
[30] Maaroufi N, Jalleli. C, Kwabia Tchana F, Landsheere X and Aroui H. Absolute line intensities and first measurements of self-collisional broadening and shift coefficients in the $2\nu_4$ band of NH_3. J Mol Spectrosc 2018;**354**:24-31.
[31] Wartewig S. IR and Raman spectroscopy: fundamental processing. Weinheim: Wiley-VCH 2003.
[32] Mertz L. Transformations in optics. New York: Wiley:1965.
[33] Carleer MR. A Windows program to accurately measure the line intensities of high-resolution Fourier transform spectra, Remote sensing of clouds and the atmosphere V 2001;**4168**:337-43.
[34] Sharpe S, Johnson T, Sams R, Chu RP, Rhoderick G, Johnson P. Gas-phase databases for quantitative infrared spectroscopy. Appl Spectrosc 2004;**58**:1452–61.
[35] Ballard J, Knight RJ, Vander Auwera J, Herman M , Di Lonardo G, Masciarelli G, Nicolaisen FM, Beukes JA, Christensen LK, McPheat R, Duxbury G, Freckle- ton R, Shine KP. An intercomparison of laboratory measurements of absorption cross-sections and integrated absorption intensities for HCFC-22. JQSRT 2000;**66**:109–28 .
[36] Pine AS. N_2 and Ar broadening and line mixing in the P and R branches of the ν_3 band of CH_4. JQSRT 1997;**57**:157-76.
[37] Weissman S. Estimation of diffusion coefficients from viscosity measurements: Polar and polyatomic gases. J Chem Phys 1964;**40**:3397-3406.